sustainability

MDPI

Article

Receding Galerkin Optimal Control with High-Order Sliding Mode Disturbance Observer for a Boiler-Turbine Unit

Gang Zhao, Yuge Sun, Zhi-Gang Su * and Yongsheng Hao

The National Engineering Research Center of Power Generation Control and Safety, School of Energy and Environment, Southeast University, Nanjing 210018, China; zhaogang@seu.edu.cn (G.Z.)
* Correspondence: zhigangsu@seu.edu.cn

Abstract: The control of the boiler-turbine unit is important for its sustainable and robust operation in power plants, which faces great challenges due to the control unit's serious nonlinearity, unmeasurable states, variable constraints, and unknown time-varying lumped disturbances. To address the above issues, this paper proposes a receding Galerkin optimal controller with a high-order sliding mode disturbance observer in a composite scheme, in which a high-order sliding mode disturbance observer is first employed to estimate the lumped disturbances based on a deviation form of the mathematical model of the boiler-turbine unit. Subsequently, under the hypothesis of state constraint, a receding Galerkin optimal controller is designed to compensate the lumped disturbances by embedding their estimates into the mathematically based predictive model at each sampling time instant. With the help of an interpolation polynomial, Gauss integration, and nonlinear solvers, an optimal control law is then obtained based on a Galerkin optimization algorithm. Consequently, disturbance rejection, target tracking, and constraint handling performance of a controlled closed-loop system are improved. Some simulation cases are conducted on a mathematical boiler-turbine unit model to demonstrate the effectiveness of the proposed method, which is supported by the quantitative result analysis, such as tracking and disturbance rejection performance indexes.

Keywords: Galerkin optimal control; boiler-turbine unit; high-order sliding mode disturbance observer

Citation: Zhao, G.; Sun, Y.; Su, Z.-G.; Hao, Y. Receding Galerkin Optimal Control with High-Order Sliding Mode Disturbance Observer for a Boiler-Turbine Unit. *Sustainability* **2023**, *15*, 10129. https://doi.org/10.3390/su151310129

Academic Editors: Bo Yang, Zhijian Liu and Lin Jiang

Received: 9 May 2023
Revised: 16 June 2023
Accepted: 22 June 2023
Published: 26 June 2023

1. Introduction

The boiler-turbine unit is the core of a thermal power plant as it produces the motive power to drive the generator. Thus, it is imperative to maintain safe and stable operation of the boiler-turbine unit. The research on boiler-turbine control methods is directly relevant to sustainability as it enables the optimization of power plant energy systems, leading to improved energy efficiency, sustainable operation, and reduced environmental impact. The control goal of the boiler-turbine unit is to meet the load demand of the electric power grid while also maintaining stable operation parameters [1]. Thereafter, control methods usually contribute to a more sustainable approach to power generation and daily automation operations. However, in practice, the boiler-turbine units are multi-input, multi-output (MIMO) nonlinear systems with multiple physical constraints and unmeasurable disturbances simultaneously. Moreover, the boiler-turbine units are now required to run over large-scale loads to adapt renewable energy power generation [2]. These all bring great challenges to the design of controllers for the boiler-turbine units with proper control performance.

Among the existing advanced controller methods applied for boiler-turbine units, the proportional-integral-differential (PID) [3] is extensively applied because of its robustness and ease of tuning. However, the control performance of PID is not satisfactory under a large-scale tracking scenario. To deal with the problem, some other advanced control approaches have been investigated in tracking conditions in recent years, including nonlinear control [4,5], gain scheduling control [6], adaptive control [7], robust control [8], and so on.

The emphasis on robust control shifts to enhancing the robustness index of the control system with plant uncertainties and external disturbances. In [9–11], fault-tolerant control methods can enhance the control system's tolerance by adaptively adjusting the control parameters through the information of fault diagnosis systems. Nevertheless, these control methods can't deal with the variable constraints directly. This obstacle leads to the investigation of several optimal controllers by minimizing a pre-defined performance index [12–17], in which model predictive control (MPC) is the prevailing one owing to its powerful abilities in addressing multiple variables, physical constraints, and tracking conditions.

Most of the aforementioned optimal controllers were designed based on either the black-box nonlinear model identified from the running data of the unit or linear models obtained by linearizing the unit's mathematical model. Thus, the nonlinearity contained in the information is discarded and not fully explored. Recently, more attention has been paid to designing optimal controllers based on the unit's mathematical model directly, and the pseudospectral (PS) method is an efficient one to solve the state- and control-constrained nonlinear optimal control problem (OCP) [18,19]. The main idea of the PS method is to transform the optimal control problem (OCP) into a nonlinear programming problem (NLP) [20], then use the NLP solver to solve out the optimal control sequence. In order to reduce the discretization error and obtain more accurate solutions, the Galerkin optimal control method [21,22] was proposed, in which the weak integral formulation is introduced to discretize the differential equations.

Considering the given merits, an adaptively receding Galerkin optimal controller (ARGOC) was proposed for a boiler-turbine unit with some unmeasured states and variable constraints in our previous work [23]. In the ARGOC, a state observer is first designed to estimate the key unmeasured state. Then, a receding Galerkin optimal controller is constructed by sufficiently taking information estimated and measured at each sampling time into account and borrowing the basic idea of receding optimization and feedback correction strategies from MPC. Thereafter, an independent model is embedded into the receding Galerkin controller structure to estimate and thus eliminate the constant disturbances in the output channels.

Nevertheless, the ARGOC fails when confronted with time-varying and state channel disturbances (i.e., lumped disturbances), which are more common in the boiler-turbine units than constant disturbances at the output channel. Under these circumstances, it is imperative to design a receding Galerkin optimal-based controller to deal with time-varying lumped disturbances. There are some difficulties in designing such a controller. The first is how to estimate the lumped disturbances in the presence of the unmeasurable state variable, fluid density, in the drum of the unit. In recent years, the disturbance observer (DO) [24–26] and the extended state observer (ESO) [27–29] have been proven to be efficient in estimating lumped disturbances in control systems. The main advantage of DO and ESO is that the disturbance observer can estimate the lumped disturbances without distinguishing whether they are external or internal. The time-varying disturbance reduction in the state channel is more focused on in this paper. Further, the disturbance observer convergence rate and accuracy, as well as the observer structure described above, still have improvement space.

The second difficulty lies in how to compensate the disturbance estimation into the receding Gakerkin optimal-based controller in an active manner. There are several disturbance compensation mechanisms in the optimal control field. In [30,31], a real-time updated equilibrium according to the disturbances and set-points is calculated first to transfer the aim of disturbance rejection and set-point tracking to the updated equilibrium. In [32], a disturbance model is added to the predictive model to compress the adverse effect of lumped disturbances. These disturbance rejection methods are not compensated by the disturbance observer in the manner of a model-predictive-based optimization process.

Motivated by the above statements, we aim to propose a receding Galerkin optimal control with a high-order sliding mode disturbance observer for a nonlinear boiler-turbine unit in a composite manner. The composite controller comprises a Galerkin optimal

control-based feedback control part and a DO-based feedforward control part. The main contributions of the composite controller are summarized as follows:

(1) A high-order sliding mode disturbance observer is designed to estimate the lumped disturbances based on the derived deviation form of the mathematical model of the boiler-turbine unit, which aims at the MIMO system and additionally addresses the observer gain tuning of the unit.
(2) The estimates of the lumped disturbances are integrated into the predictive model and then feedforward compensated in the Galerkin optimal control-based feedback channel. As will be anticipated, the proposed composite controller exhibits superior time-varying lumped disturbance rejection and target tracking performance for a boiler-turbine unit.

The rest of the paper is organized as follows: The mathematical model of a disturbed boiler-turbine unit and problem statement are given in Section 2. Section 3 presents the methodology of the proposed composite controller. Simulation studies are carried out in Section 4 to verify the superiority of our proposed controller in time-varying lumped disturbance rejection and set-point tracking. The last section concludes this paper.

2. Disturbed Boiler-Turbine Unit and Problem Statement

In this paper, a 160 MW oil-fired drum-type boiler-turbine unit is considered 1, whose flow diagram is summarized in Figure 1. The mathematical model of this unit has been established in the form of

$$\begin{cases} \dot{x}_1 = f_1(x,u) := -a_1 u_2 x_1^{1.125} + a_2 u_1 - a_3 u_3 + \bar{d}_1(t), \\ \dot{x}_2 = f_2(x,u) := (b_1 u_2 - b_2) x_1^{1.125} - x_2 + \bar{d}_2(t), \\ \dot{x}_3 = f_3(x,u) := (c_1 u_3 - (c_2 u_2 - c_3) x_1)/c_4 + \bar{d}_3(t), \\ y_1 = x_1, \\ y_2 = x_2, \\ y_3 = h(x,u) := 0.05(0.13073 x_3 + 100\alpha_{cs} + (q_e/9 - 67.975)), \end{cases} \tag{1}$$

where the state variables x_1, x_2 and x_3 signify drum pressure (kg/cm^2), electrical output (MW), and fluid density in the drum (kg/cm^3), respectively. The outputs are the drum steam pressure (y_1), electrical output (y_2), and drum water level (y_3). The controllable inputs u_1, u_2, and u_3 are the valve positions for fuel, steam, and feedwater flow, respectively. All the valve positions are normalized into [0, 1]. The coefficient α_{cs} and evaporation rate of steam q_e (kg/s) are defined as

$$\alpha_{cs} = \frac{(1 - 0.001538 x_3)(0.8 x_1 - 25.6)}{x_3(1.0394 - 0.0012304 x_1)} \tag{2}$$

$$q_e = (0.854 u_2 - 0.147) x_1 + 45.59 u_1 - 2.514 u_3 - 2.096 \tag{3}$$

$\bar{d}_i(t)$, $i = 1, 2, 3$ are unknown uncertainties or disturbances; referring to 33, parameters a_i, b_i, c_i do not have the physical meaning as the previous parameter, which is to be identified by the operating data, as shown in Table 1.

Table 1. Model Parameters of Boiler–Turbine Unit.

$a_1 = 0.0018$	$b_1 = 0.073$	$c_1 = 141$
$a_2 = 0.9$	$b_2 = 0.016$	$c_2 = 1.1$
$a_3 = 0.15$	$b_3 = 0.1$	$c_3 = 0.19$
		$c_4 = 85$

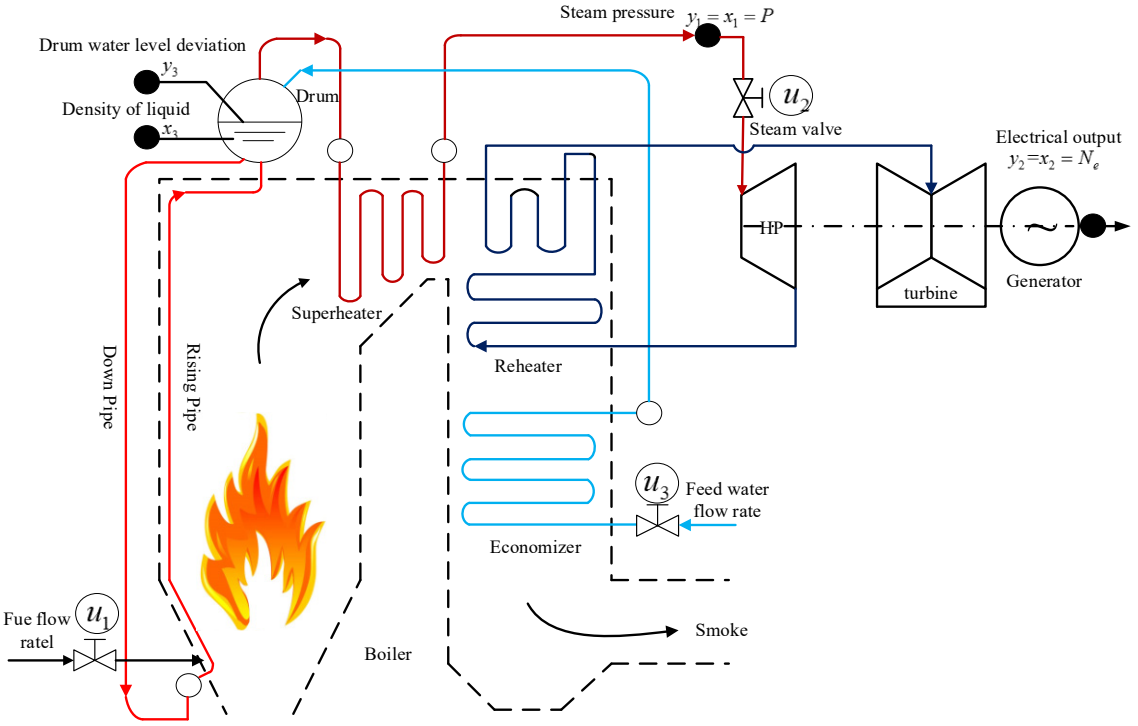

Figure 1. Structure of a 160 MW boiler-turbine unit in a thermal power plant.

Table 2 gives some typical operating points of the boiler-turbine unit in the absence of disturbances. The main control task is to regulate the outputs of the unit to track large-scale setpoints or references.

Table 2. Typical Operating Points of Boiler–Turbine Unit.

	#1	#2	#3	#4	#5	#6	#7
x_{1d}	75.6	86.4	97.2	108	118.8	129.6	135.4
x_{2d}	15.27	36.65	50.52	66.65	85.06	105.8	127
x_{3d}	299.6	324.4	385.2	428	470.8	513.6	556.4
u_{1d}	0.156	0.209	0.271	0.34	0.418	0.505	0.600
u_{2d}	0.483	0.552	0.621	0.69	0.759	0.828	0.897
u_{3d}	0.183	0.256	0.34	0.433	0.543	0.663	0.793
y_{3d}	−0.97	−0.65	−0.32	0	0.32	0.64	0.98

In order to implement the receding Galerkin optimal controller, all the states should be known in advance. However, the state variable x_3, that is the fluid density in the drum, cannot be measured directly. In this case, we adopt the available y_3 to design the controller instead. To simplify the controller design, the last three terms in y_3 can be viewed as a disturbance term, $w(t)$, that is

$$w(t) := 0.05(100\alpha_{cs} + q_e/9 - 67.975). \tag{4}$$

Therefore, the first derivative of y_3 is

$$\dot{y}_3 = c_0\dot{x}_3 + \dot{w}(t) = c_0[c_1u_3 - (c_2u_2 - c_3)x_1]/c_4 + c_0\bar{d}_3(t) + \dot{w}(t), \tag{5}$$

where constant $c_0 = 0.00654$.

It is observable from (1) that there is a rate of change constraint on the control inputs, which is expected to be introduced into the system dynamics for improving control performance. Define $v_1 = \dot{u}_1/c_1$, $v_2 = \dot{u}_2/c_2$, $v_3 = \dot{u}_3/c_3$ with expansion coefficients c_1, c_2,

c_3. Then, by given the setpoints/references y_{id} and their first derivatives $\dot{y}_{id}$ and defining outputs errors $z_i = y_i - y_{id}$, $i = 1, 2, 3$, dynamics are retrofitted as

$$\begin{aligned}
\dot{z}_1 &= -a_1 u_2 (z_1 + y_{1d})^{1.125} + a_2 u_1 - a_3 u_3 - \dot{y}_{1d} + d_1, \\
\dot{z}_2 &= (b_1 u_2 - b_2)(z_1 + y_{1d})^{1.125} - b_3 (z_2 + y_{2d}) - \dot{y}_{2d} + d_2, \\
\dot{z}_3 &= c_0 [c_1 u_3 - (c_2 u_2 - c_3)(z_1 + y_{1d})]/c_4 - \dot{y}_{3d} + d_3, \\
\dot{u}_1 &= c_1 v_1, \\
\dot{u}_2 &= c_2 v_2, \\
\dot{u}_3 &= c_3 v_3.
\end{aligned} \tag{6}$$

where the lumped disturbances are

$$d_i(t) := \begin{cases} \overline{d}_i(t) & i = 1, 2, \\ c_0 \overline{d}_3(t) + \dot{w}(t) & i = 3, \end{cases} \tag{7}$$

which satisfies the following assumption.

Assumption 1. *The lumped disturbances d_i satisfy $\left| d_i^{(j)} \right| \leq \varsigma_i$, where $j = 1, 2, \ldots, L$ with a positive integer $L \leq 3$ and positive constants ς_i, $i = 1, 2, 3$.*

Correspondingly, for safety consideration, model (1) should satisfy the following constraints [1, 5], which are restated as

$$\begin{aligned}
&70 \leq x_1 \leq 150,\ 10 \leq x_2 \leq 190,\ 0 \leq u_1, u_2, u_3 \leq 1, \\
&|v_1| \leq 0.007/c_1, |v_2| \leq 0.02/c_2, |v_3| \leq 0.05/c_3, \\
&h(x, u) - 1 \leq 0, h(x, u) + 1 \geq 0.
\end{aligned} \tag{8}$$

Dynamics (6)–(8) are utilized to design the composite controller, to which we turn next.

3. Main Results: Method

This section includes a concise and precise description of the proposed method design, their interpretation, as well as results that can be drawn.

3.1. High-Order Sliding Mode Disturbance Observer Design

A high-order sliding mode disturbance observer developed in [33–36] is normally used for the single-input-single-output (SISO) n-th order differential dynamics, while in this research it has tentatively been employed for the MIMO system (6) to estimate the unknown lumped disturbances as

$$\begin{aligned}
\dot{\xi}_0^i &= v_0^i + f_i\left(z, u, y_{id}, \dot{y}_{id}\right), \\
v_0^i &= -\lambda_0^i L_i^{\frac{1}{L+1}} \left| \xi_0^i - z_i \right|^{\frac{1}{L+1}} \operatorname{sign}\left(\xi_0^i - z_i\right) + \xi_1^i, \\
\dot{\xi}_1^i &= v_1^i, \\
v_1^i &= -\lambda_1^i L_i^{\frac{1}{L}} \left| \xi_1^i - v_0^i \right|^{\frac{L-1}{L}} \operatorname{sign}\left(\xi_1^i - v_0^i\right) + \xi_2^i, \\
&\vdots \\
\dot{\xi}_l^i &= v_l^i, \\
v_l^i &= -\lambda_l^i L_i^{\frac{1}{L+1-l}} \left| \xi_l^i - v_{l-1}^i \right|^{\frac{L-l}{L+1-l}} \operatorname{sign}\left(\xi_l^i - v_{l-1}^i\right) + \xi_l^i, \\
&\vdots \\
\dot{\xi}_L^i &= v_L^i, \\
v_L^i &= -\lambda_L^i L_i \operatorname{sign}\left(\xi_L^i - v_{L-1}^i\right),
\end{aligned} \tag{9}$$

where L_i, λ_l^i, $i = 1, 2, 3$, $l = 0, 1, \ldots, L$ are observer coefficients and sign $(\cdot)$ is a sign function. Accordingly, $\xi_0^i, \xi_1^i, \xi_2^i, \ldots, \xi_L^i$ are, respectively, the estimates $\hat{z}_i, \hat{d}_i, \hat{\dot{d}}_i, \ldots \hat{d}_i^{(L-1)}$.

Define observer errors as $e_0^i = \xi_0^i - z_i, e_l^i = \xi_l^i - d_i^{(l-1)}$, l = 1, 2, 3, with $d_i^0 = d_i$ and $d_i^{(l-1)}$ the (l-1)th derivative of d_i. The observer error dynamics can be derived from (6) and (9) as

$$\begin{aligned} \dot{e}_0^i &= -\lambda_0^i L_i^{1/4} \left|e_0^i\right|^{3/4} \mathrm{sign}\left(e_0^i\right) + e_1^i, \\ \dot{e}_1^i &= -\lambda_1^i L_i^{1/3} \left|e_1^i - \dot{e}_0^i\right|^{2/3} \mathrm{sign}\left(e_1^i - \dot{e}_0^i\right) + e_2^i, \\ \dot{e}_2^i &= -\lambda_2^i L_i^{1/2} \left|e_2^i - \dot{e}_1^i\right|^{1/2} \mathrm{sign}\left(e_2^i - \dot{e}_1^i\right) + e_3^i, \\ \dot{e}_3^i &\in -\lambda_3^i L_i \mathrm{sign}\left(e_3^i - \dot{e}_2^i\right) + [-\varsigma_i, \varsigma_i]. \end{aligned} \tag{10}$$

It can be concluded from 34–36 that the observer error is finite-time stable. That is, there exists a finite time t^*, such that $e_0^i \equiv 0$, $e_1^i \equiv 0$, $e_2^i \equiv 0$, $e_3^i \equiv 0$ when $t > t^*$.

Remark: The nature of HOSM is a differentiator that uses known information from system (6) to mathematically reconstruct an unknown disturbance. HOSM is the preliminary part for the whole composite controller design, which has significance for the reduction of disturbances caused by model uncertainties and coupling terms in (6). With this foreshadowing, the estimate information of all disturbances is embedded into the model (9) and restored as the nominal one for the rolling optimization process to calculate the control law.

3.2. Galerkin Optimal Control Design

The optimal control problem based on mathematical model (6) can be described as follows: determine the state-control function pair, $t \to (z, u) \in R^{N_z} \times R^{N_u}$ to minimize the following cost function

$$\begin{aligned} &\min_{z,u,v} J_{BT} = \int_{t_0}^{t_f} \left[z^{\mathrm{T}} P z + v^{\mathrm{T}} Q v\right] dt \\ &\quad s.t. \quad (9),\ (10), \end{aligned} \tag{11}$$

where $z = [z_1,\ z_2,\ z_3]^{\mathrm{T}}$, $v = [v_1,\ v_2,\ v_3]^{\mathrm{T}}$, $P = diag\{p_1,\ p_2,\ p_3\}$, $Q = diag\{q_1,\ q_2,\ q_3\}$.

To solve the optimal control problem (11), a Galerkin optimal method is first designed to transform (11) into a nonlinear programming problem (NLP), which can then be computed by several sequential quadratic programming (SQP) software packages such as SNOPT [37] with high computational efficiency. To be specific, the Galerkin optimal method is performed in the following four steps: approximating state and control variables, discretizing the system dynamics and variable constraints, and integrating the cost function via interpolation polynomial [38,39] and Gauss integration [23] on a series of Legendre-Gauss-Lobatto (LGL) nodes. The LGL nodes are calculated as the roots of

$$\xi(\tau) = \left(1 - \tau^2\right) \dot{L}_N(\tau), \tag{12}$$

where $L_N(\tau)$ is the Nth order Legendre polynomial defined by

$$L_N(\tau) := \frac{(-1)^N}{2^N N!} \frac{d^N}{d\tau^N} \left(1 - \tau^2\right)^N. \tag{13}$$

Totally, there are $(N+1)$ LGL nodes in τ-space as $\{\tau_i\}_{i=0}^N$ $(\tau_0 = -1 < \tau_1 < \tau_2 < \cdots < \tau_N = 1)$. By converting the real-time domain $t \in [\ t_0,\ t_f\ ]$ into a closed interval $\tau \in [-1,1]$ according to

$$\tau = \frac{2t - (t_f + t_0)}{t_f - t_0}, \tag{14}$$

one can get corresponding point $\{t_i\}_{i=0}^{N}$, $\left(t_0 = t^{N_0} < t^{N_1} < t^{N_2} < \cdots < t^{N_N} = t_f\right)$ in the real-time domain.

With the help of LGL nodes, the Galerkin method approximates the state and control variables by the Nth-order Lagrange interpolation polynomial defined on LGL nodes as follows:

$$z(\tau) \approx \sum_{j=0}^{N} \phi_j^N(\tau) \cdot z^{N_j}, \tag{15}$$

$$u(\tau) \approx \sum_{j=0}^{N} \phi_j^N(\tau) \cdot u^{N_j}, \tag{16}$$

where z^{N_j} and u^{N_j} are the state and control variables at the LGL nodes τ_j. $\phi_j^N(\tau)$ is the N-th order Lagrange interpolation basis function defined by $\phi_j^N(\tau) = \prod_{i=0.i\neq j}^{N} \frac{\tau-\tau_i}{\tau_j-\tau_i}$.

Using (15) and (16), the differential equation can be approximated using the following integral formulation

$$\int_{-1}^{1} \psi_i(\tau)\left(\dot{z}(\tau) - \frac{t_f - t_0}{2} f(z(\tau), u(\tau))\right) d\tau = 0 \tag{17}$$

with test functions $\psi_i(\tau)$. Equation (17) can be further rewritten as (18) when $\psi_i(\tau)$ is denoted as the basis function $\phi_j^N(\tau)$,

$$\sum_{j=0}^{N} \underbrace{\int_{-1}^{1} \phi_i^N(\tau)\dot{\phi}_j^N(\tau) d\tau}_{D_{ij}} \cdot z^{N_j} - \underbrace{\frac{t_f - t_0}{2} \int_{-1}^{1} \phi_i^N(\tau) f(z(\tau), u(\tau)) d\tau}_{\Delta_i} = 0. \tag{18}$$

For simplicity, the D_{ij} and Δ_i can be approximated as

$$D_{ij} \approx \sum_{k=0}^{N} \phi_i^N(\tau_k)\dot{\phi}_j^N(\tau_k)\omega_k \approx \dot{\phi}_j^N(\tau_i)\omega_i = A_{ij}\omega_i \tag{19}$$

$$\Delta_i \approx \frac{t_f - t_0}{2} f(z(\tau_i), u(\tau_i))\omega_i \tag{20}$$

where A_{ij} is the Legendre differentiation matrix calculated by

$$A_{ij} = \begin{cases} \frac{L_N(\tau_i)}{L_N(\tau_j)} \frac{1}{\tau_i - \tau_j}, & i \neq j, \\ \frac{-N(N+1)}{4}, & i = j = 0, \\ \frac{N(N+1)}{4}, & i = j = N, \\ 0, & i = j \in [1, \cdots, N-1]. \end{cases} \tag{21}$$

ω_i, $i = 0, 1, \ldots, N$, are the quadrature weights, and the LGL version of quadrature weights is utilized in the present paper, which is calculated as

$$\omega_i = \frac{2}{N(N+1)[L_N(\tau_i)]}, i = 0, 1, \ldots, N. \tag{22}$$

With the D_{ij} in (19) and Δ_i in (20), the dynamics (18) can thus be finally simplified as

$$\begin{aligned} &\sum_{j=0}^{N} D_{ij} \cdot z_k^j - \Delta_{ki} = 0, \quad i = 0, 1, \cdots, N, \quad k = 1, \quad 2, \quad 3, \\ &\sum_{j=0}^{N} D_{ij} \cdot u_k^j - \Delta_{(k+3)i} = 0, \quad i = 0, 1, \cdots, N, \quad k = 1, \quad 2, \quad 3, \end{aligned} \tag{23}$$

where

$$\begin{aligned}
\Delta_{1i} &= \tfrac{t_f-t_0}{2}\Big(-a_1u_2^i(z_1^i+y_{1d})^{1.125}+a_2u_1^i-a_3u_3^i-\dot{y}_{1d}+\xi_0^1\Big)w_i,\\
\Delta_{2i} &= \tfrac{t_f-t_0}{2}\Big((b_1u_2^i-b_2)(z_1^i+y_{1d})^{1.125}-b_3(z_2^i+y_{2d})-\dot{y}_{2d}+\xi_0^2\Big)w_i,\\
\Delta_{3i} &= \tfrac{t_f-t_0}{2}\big(c_0\left[c_1u_3^i-(c_2u_2^i-c_3)(z_1^i+y_{1d})\right]/c_4-\dot{y}_{3d}+\xi_0^3\big)w_i,\\
\Delta_{4i} &= \tfrac{t_f-t_0}{2}(c_1v_1^i)w_i,\\
\Delta_{5i} &= \tfrac{t_f-t_0}{2}(c_2v_2^i)w_i,\\
\Delta_{6i} &= \tfrac{t_f-t_0}{2}(c_3v_3^i)w_i.
\end{aligned}$$

The variable constraints (10) can be discretized as

$$\begin{aligned}
&-10\le z_1^i\le 10,\quad -10\le z_2^i\le 10,\quad -1\le z_3^i\le 1,\quad i=0,1,\cdots,N\\
&0\le\left|u_1^i\right|\le 1,\quad 0\le\left|u_2^i\right|\le 1,\quad 0\le\left|u_3^i\right|\le 1,\quad i=0,1,\cdots,N\\
&\left|v_1^i\right|\le 0.007/c_1,\left|v_2^i\right|\le 0.02/c_2,\left|v_3^i\right|\le 0.05/c_3,\quad i=0,1,\cdots,N
\end{aligned}\tag{24}$$

In a relatively easy way, the cost function (11) is approximated according to the Gauss–Lobatto integration rule as follows:

$$\begin{aligned}
J &= \textstyle\int_{t_0}^{t_f}\left[z^{\mathrm{T}}Pz+v^{\mathrm{T}}Qv\right]dt\\
&\approx \tfrac{t_f-t_0}{2}\sum_{j=0}^{N}\left[p_1\left(z_1^{N_j}\right)^2+p_2\left(z_2^{N_j}\right)^2+p_3\left(z_3^{N_j}\right)^2+q_1\left(v_1^{N_j}\right)^2+q_2\left(v_2^{N_j}\right)^2+q_3\left(v_3^{N_j}\right)^2\right]w_j.
\end{aligned}\tag{25}$$

Therefore, the continuous optimal control problem (13) can be constructed as

$$\begin{aligned}
J &= \tfrac{t_f-t_0}{2}\sum_{j=0}^{N}\left[p_1\left(z_1^j\right)^2+p_2\left(z_2^j\right)^2+p_3\left(z_3^j\right)^2+q_1\left(v_1^j\right)^2+q_2\left(v_2^j\right)^2+q_3\left(v_3^j\right)^2\right]w_j,\\
s.t.\quad &\left\|\sum_{j=0}^{N}D_{ij}\cdot z_k^j-\Delta_{ki}\right\|_\infty\le\delta^N,\quad i=0,1,\cdots,N,\quad k=1,\ 2,\ 3,\\
&\left\|\sum_{j=0}^{N}D_{ij}\cdot u_k^j-\Delta_{(k+3)i}\right\|_\infty\le\delta^N,\quad i=0,1,\cdots,N,\quad k=1,\ 2,\ 3.\\
&-10\le z_1^i\le 10,\quad -10\le z_2^i\le 10,\quad -1\le z_3^i\le 1,\quad i=0,1,\cdots,N\\
&0\le\left|u_1^i\right|\le 1,\quad 0\le\left|u_2^i\right|\le 1,\quad 0\le\left|u_3^i\right|\le 1,\quad i=0,1,\cdots,N\\
&\left|v_1^i\right|\le 0.007/c_1,\left|v_2^i\right|\le 0.02/c_2,\left|v_3^i\right|\le 0.05/c_3,\quad i=0,1,\cdots,N,
\end{aligned}\tag{26}$$

where δ^N is a constant tolerance used to guarantee the feasibility of the NLP (26).

3.3. Receding Galerkin Optimal Control Design with High-Order Sliding Mode Disturbance Observer

It is evident that the Galerkin method interpreted in Section 3.2 is only feasible for the stabilization problem rather than the tracking problem. To deal with the tracking problem, the useful information at each sampling instant should be taken into account, including the information of states, outputs, and references. To address this problem, a receding version of Galerkin's optimal control strategy with a high-order sliding mode disturbance observer in a composite way is proposed by borrowing the basic idea from model predictive control (MPC) and is explained as follows:

(i). At current time instant t_k, the lumped disturbances of system (9) are estimated by the high-order sliding mode disturbance observer (11) as $\xi_0^1,\ \xi_0^2,\ \xi_0^3$.

(ii). Let the current state $z(t_k)$ and control $u(t_k)$ be the initial conditions, that is, $z_{0,k}=z(t_k)$, $u_{0,k}=u(t_k)$. Then embed the obtained $\xi_0^1,\ \xi_0^2,\ \xi_0^3$ into the nonlinear mathematical model based-predictive model, the optimal discrete state and control sequences $\left\{z^{j,k}\right\}_{j=0}^{N}$ and $\left\{u^{j,k}\right\}_{j=0}^{N}$ can be acquired by minimizing J_{BT} in (29) through

the Galerkin optimal control method over the prediction horizon $[t_0, t_f]$: = $[t_k, t_k + \Delta T]$,

$$\begin{aligned} &\min_{\{x^{j,k},u^{j,k},v^{j,k}\}} J_{BT} = \tfrac{\Delta T}{2}\sum_{j=0}^{N}\left[(z^{j,k})^{\mathrm{T}}P(z^{j,k}) + (v^{j,k})^{\mathrm{T}}Qv^{j,k}\right]w_j, \\ &s.t. \left\|\sum_{j=0}^{N} D_{i,j}z^{j,k} - \Delta_i\right\|_{\infty} \le \delta^N, \\ &\quad \|z^{0,k} - z(t_k)\|_{\infty} \le \delta^N, \\ &\quad \|u^{0,k} - u(t_k)\|_{\infty} \le \delta^N, \end{aligned} \tag{27}$$

$$\begin{aligned} &-10 \le z_1^i \le 10, \quad -10 \le z_2^i \le 10, \quad -1 \le z_3^i \le 1, \quad i = 0, 1, \cdots, N \\ &0 \le \left|u_1^i\right| \le 1, \quad 0 \le \left|u_2^i\right| \le 1, \quad 0 \le \left|u_3^i\right| \le 1, \quad i = 0, 1, \cdots, N \\ &\left|v_1^i\right| \le 0.007/c_1, \left|v_2^i\right| \le 0.02/c_2, \left|v_3^i\right| \le 0.05/c_3, \quad i = 0, 1, \cdots, N, \end{aligned}$$

where ΔT is the length of horizon. D_{ij} and Δ_i are shown in (19) and in (20). To solve the discrete nonlinear programming problem (29), a nonlinear programming solver such as SNOPT is usually used 39.

(iii). Apply the optimal control law $u^{1,k}$ on the unit and repeat the above operations in steps (i) and (ii) at the coming time instant t_{k+1}. It is worth mentioning that the $u^{1,k}$ is a composite control law which contains the compensation of the lumped disturbances.

To sum up, the scheme of the proposed composite control method can be illustrated in Figure 2.

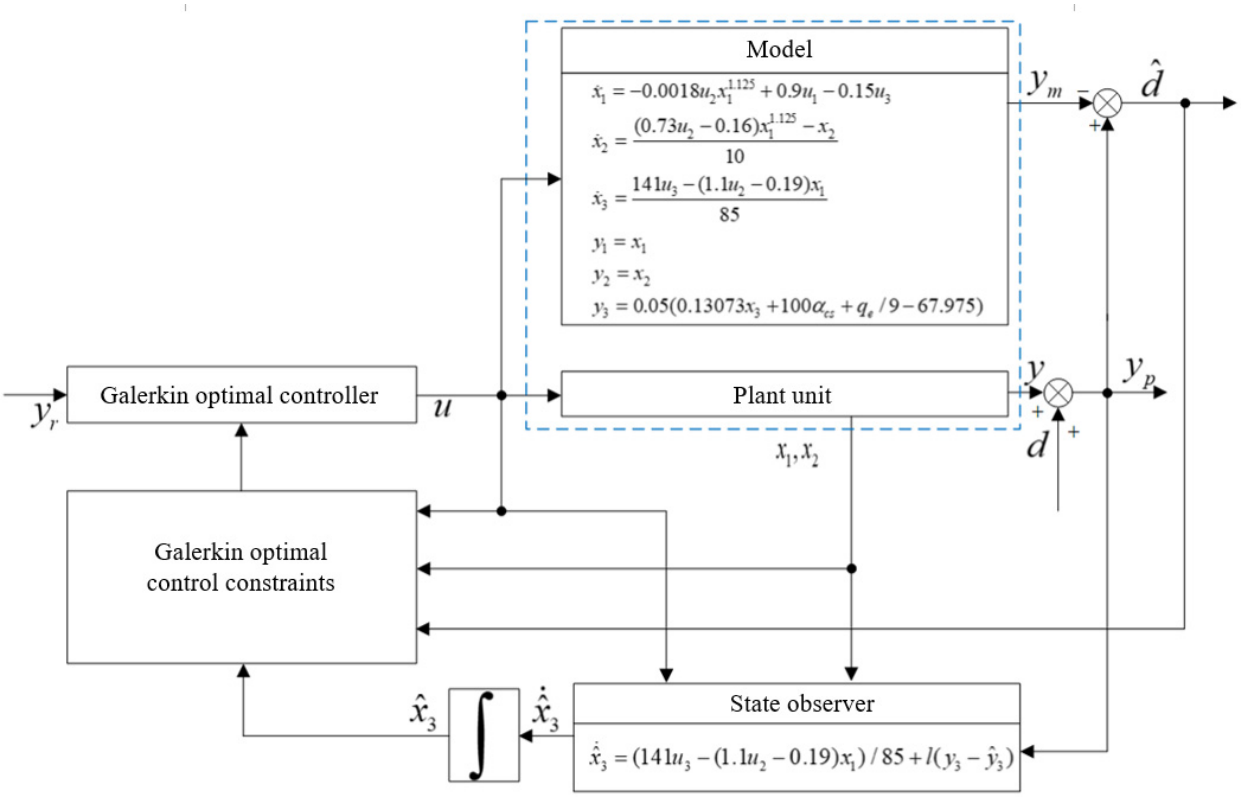

Figure 2. Block diagram of the receding Galerkin optimal controller with high-order sliding mode disturbance observer.

4. Simulations

In this section, some simulation cases are conducted to validate the performance of the proposed composite controller for the oil-fired drum-type boiler-turbine unit (1). For implementation purposes, a nonlinear programming solver SNOPT is adopted. Addition-

ally, some controller parameters should be preset such as disturbance observer parameters (λ_l^i, L_i) and controller parameters (N, c, P, Q).

4.1. Parameters Assignment

As remarked in 1 and 35, the faster the convergence of disturbance observer should be, the larger λ_l^i and L_i are usually required. In fact, if the disturbance observer converges too fast, it will lead to the violation of the constraints imposed on control inputs. With these in mind, we select $\lambda_0^i = 1.5$, $\lambda_1^i = 0.1$, $\lambda_2^i = \lambda_3^i = 0.01$, $L_i = 2$, $i = 1, 2, 3$. Moreover, we choose $N = 20$, $P = diag\{1, 1, 2000\}$, $Q = diag\{2, 1, 2\}$, $c = [0.001, 0.001, 0.001]$ according to 23.

4.2. Case 1: Wide-Range Load Tracking without Lumped Disturbances

In this case, we intend to validate the tracking performance of the proposed composite controller without lumped disturbances. The change process of the working condition point is as in Table 3:

Table 3. The change process of the working condition point.

Time Period (s)	0–400	400–1000	1000–1400	1400–2400	2400–2700	2700–3200	3200–3500
Working condition	#2	#2 to #6	#6	#6 to #1	#1	#1 to #3	#3

From Table 3, the whole simulation time period is 3500 s, and the lumped disturbances are set to zero. With the initial conditions $z_1(0) = 5$, $z_2(0) = 10$, $z_3(0) = 0.1$, and the parameters assignment as Section 4.1. Implementing the composite controller on the unit (1) resulted in simulation results Figures 3 and 4, respectively.

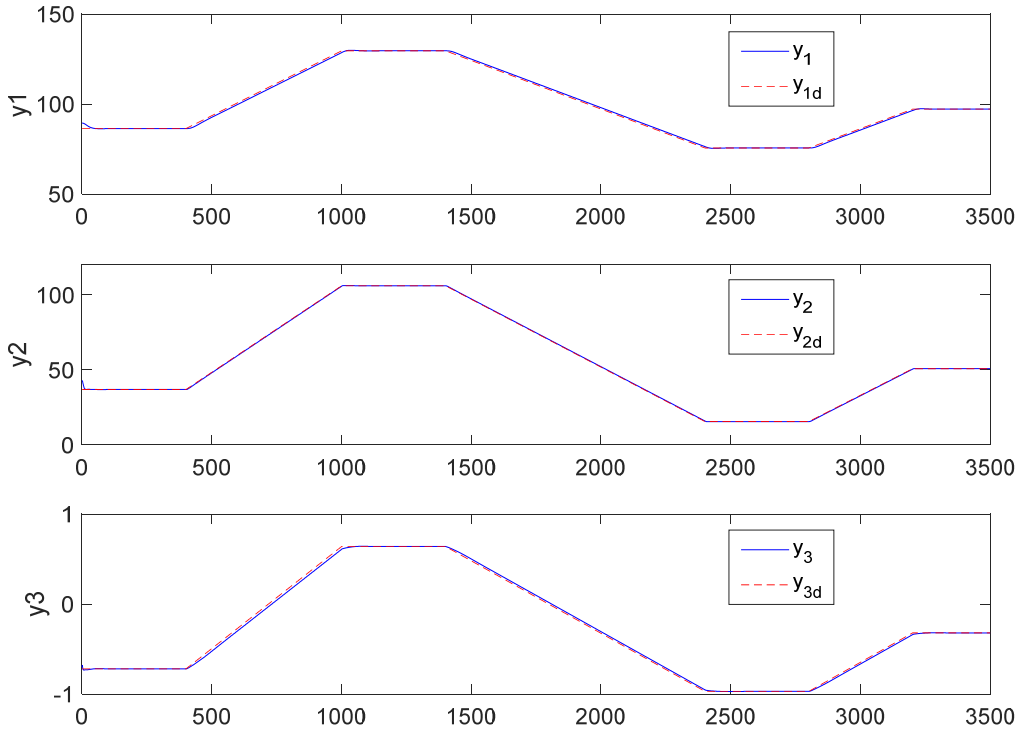

Figure 3. Outputs of the unit in the case of tracking large-scale load references.

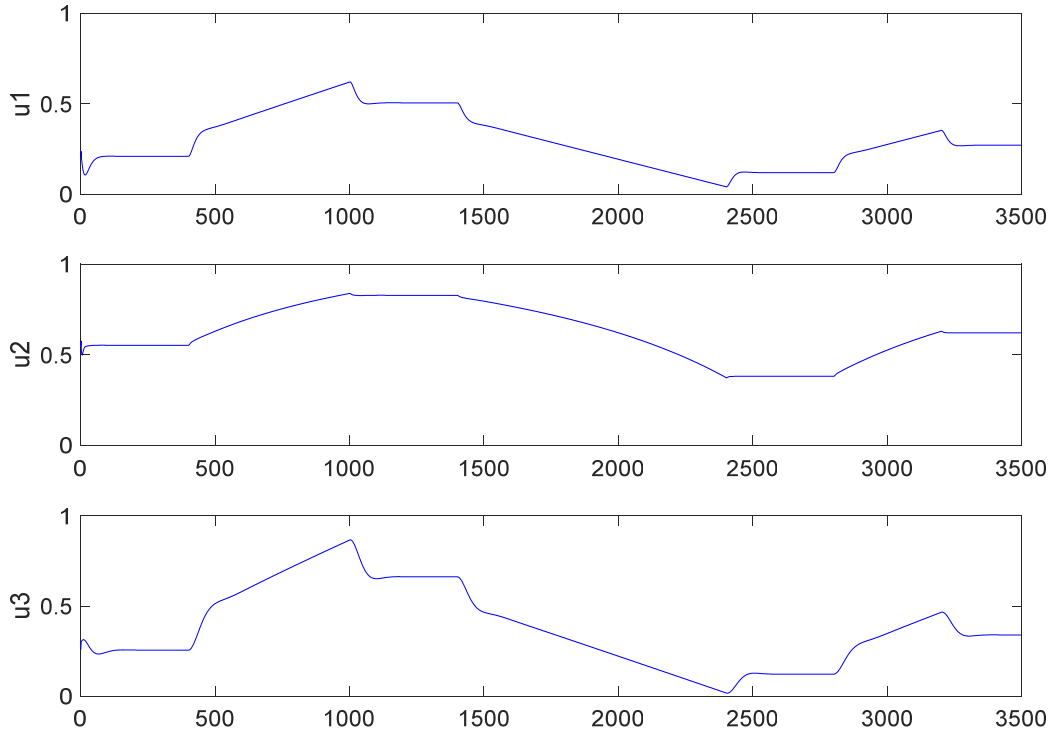

Figure 4. Control inputs of the unit in the case of tracking large-scale load references.

Figure 3 shows the output responses under control inputs in Figure 4. The x-axis is the time with its unit in seconds. It can be observed that the outputs y_i can track large-scale references y_{id} rapidly without deviation. Meanwhile, Figure 4 illustrates that all the control inputs u_i strictly meet the constraints.

4.3. Case 2: Wide-Range Load Tracking with Lumped Disturbances

In Case 1, the boiler-turbine unit is just regulated to track large-scale references without lumped disturbances. In this case, we aim to run the unit to track large-scale references in the presence of lumped disturbances $d_i(t)$ defined by

$$\begin{aligned} d_1 &:= -0.0002(z_1 + y_{1d})^{9/8}u_2 - 0.1u_1 + 0.02u_3, \\ d_2 &:= (0.01u_2 + 0.004)(z_1 + y_{1d})^{9/8} - 0.01(z_2 + y_{2d}) + 0.2\sin(0.01\pi t), \\ d_3 &:= 0.001u_3 - \left(2 \times 10^{-5}u_2 + 5 \times 10^{-6}\right)(z_1 + y_{1d}). \end{aligned} \tag{28}$$

The whole simulation time period is 3500 s, and the lumped disturbances (28) occur at the 400th second and vanish at the 3200th second. The initial conditions and parameter assignments are the same as those in Case 1. Figures 5–7 illustrate the estimates of lumped disturbances defined in (28), the response curves of the outputs y_i, and the control inputs u_i.

It can be seen in Figure 5 that the lumped disturbances can be estimated by the high-order sliding mode disturbance observer (11) with high accuracy. Based on this, Figure 6 exhibits that the outputs y_i can track large-scale references y_{id} rapidly in most cases, except for the period when drastic disturbances begin to happen or vanish. Meanwhile, it can be seen that the nominal performance can be reserved when the lumped disturbances vanish at the 2300th second. Furthermore, Figure 7 shows that the control inputs u_i change drastically due to the large-scale changes of references and the drastic lumped disturbances during time period (400, 3200), but the control inputs can be guaranteed inside the boundary [0, 1]. These all illustrate the excellent disturbance rejection and set-point tracking performance of the proposed composite control method.

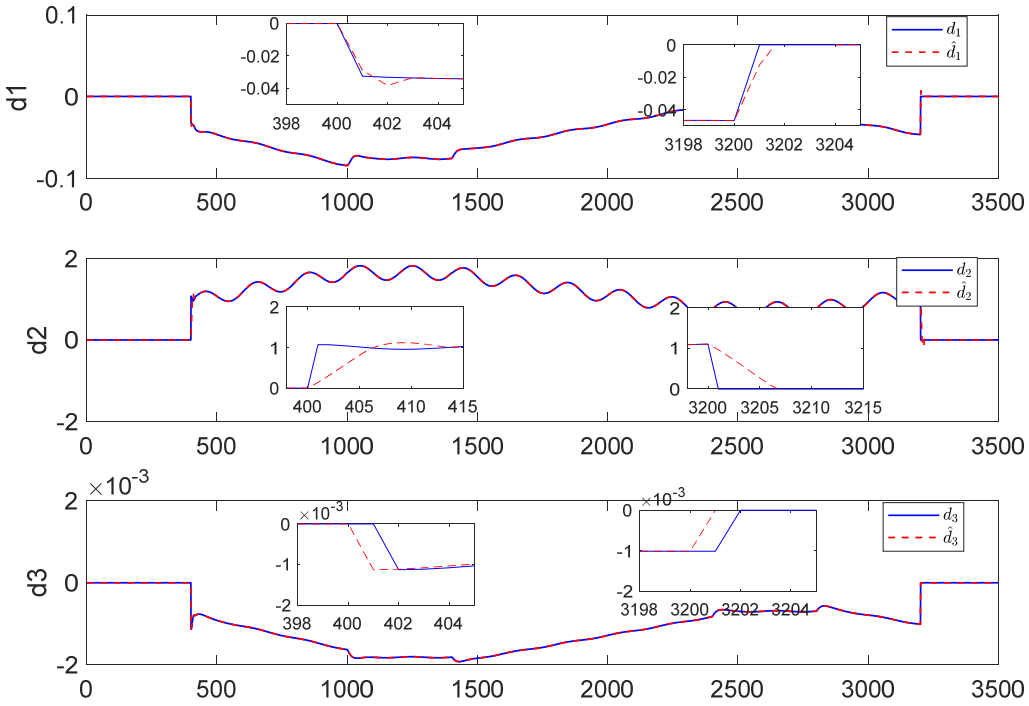

Figure 5. Estimates of lumped disturbances.

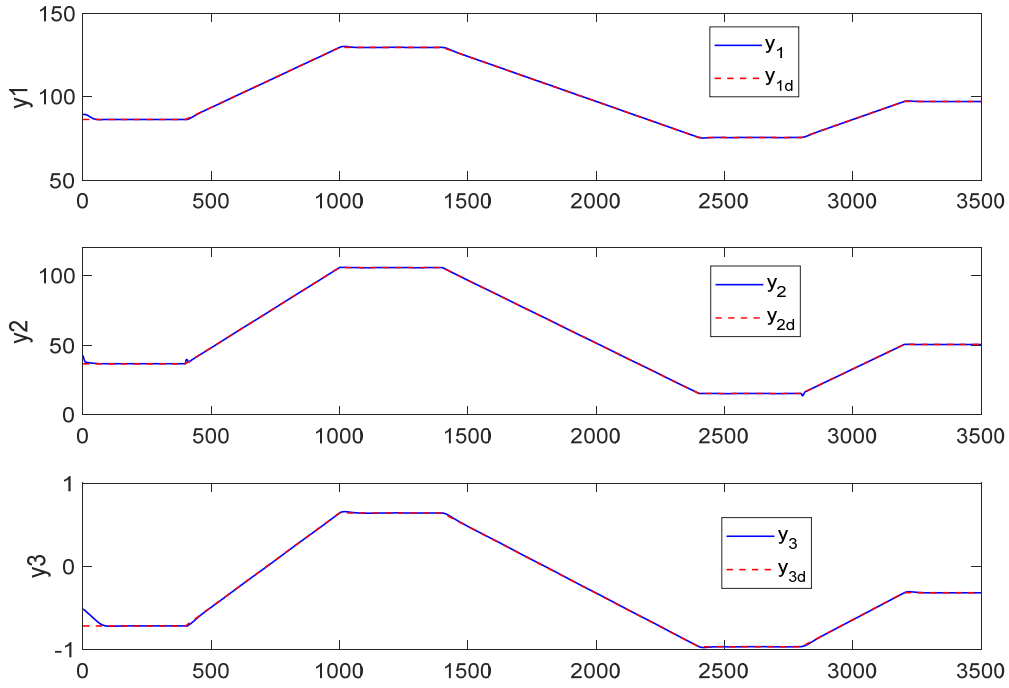

Figure 6. Output trajectories in presence of lumped disturbances.

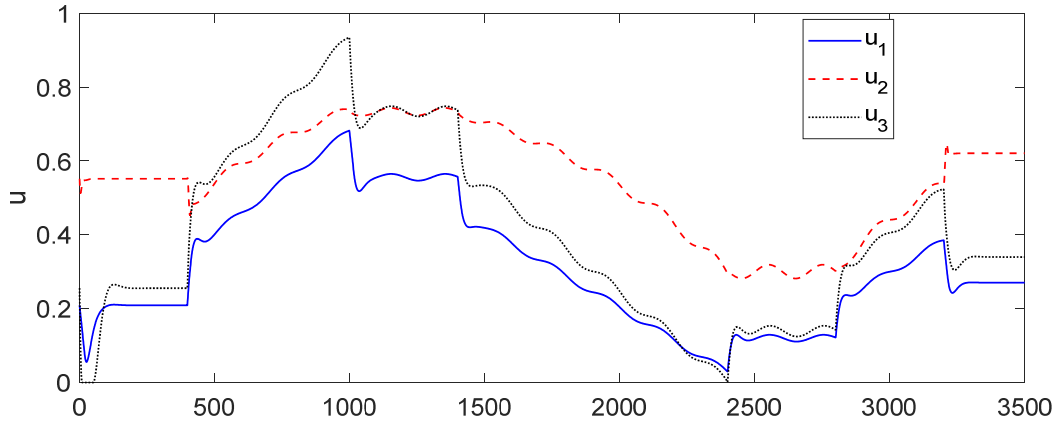

Figure 7. Control inputs curves.

4.4. Case 3: Control Performance Comparison under Wide-Range Load Tracking Conditions

To further verify the control performance of our proposed composite controller, a state feedback controller developed in 1 is carried out as the comparative method by considering its anti-disturbance ability.

The whole simulation time period is 3500 s. The lumped disturbances, initial conditions, and parameters assignment are set the same as those of Case 2. Corresponding simulation results are drawn in Figures 8 and 9.

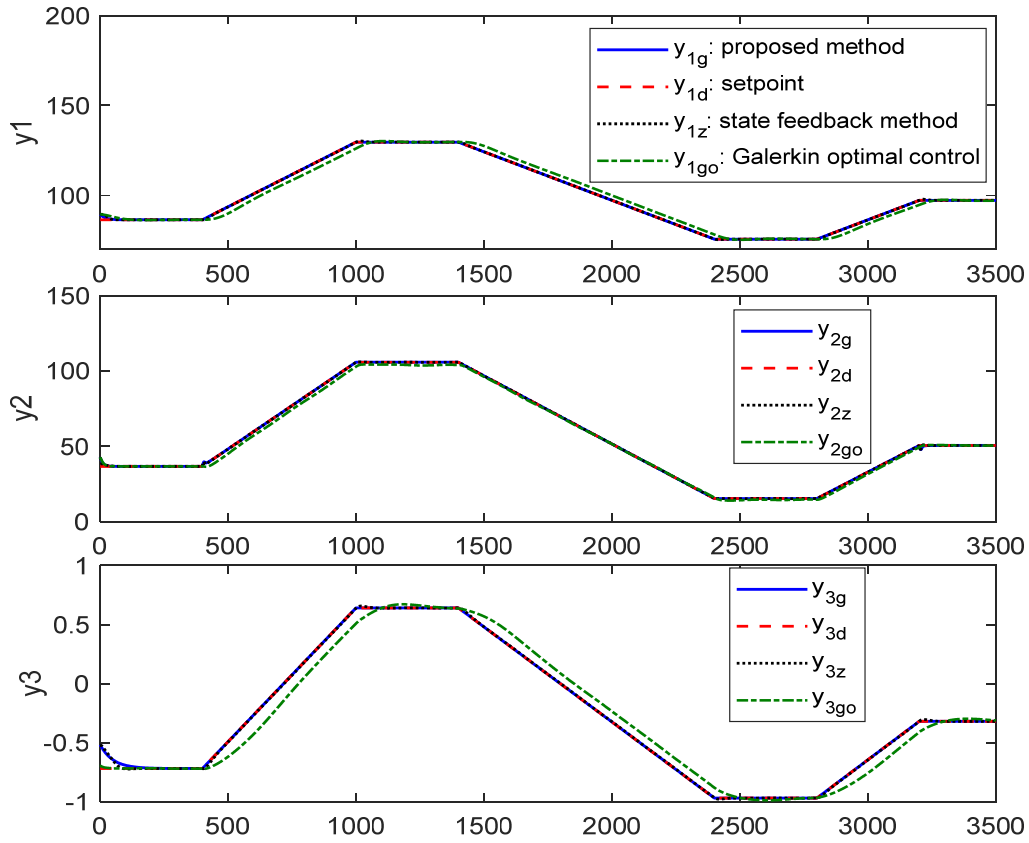

Figure 8. Control outputs in presence of lumped disturbances.

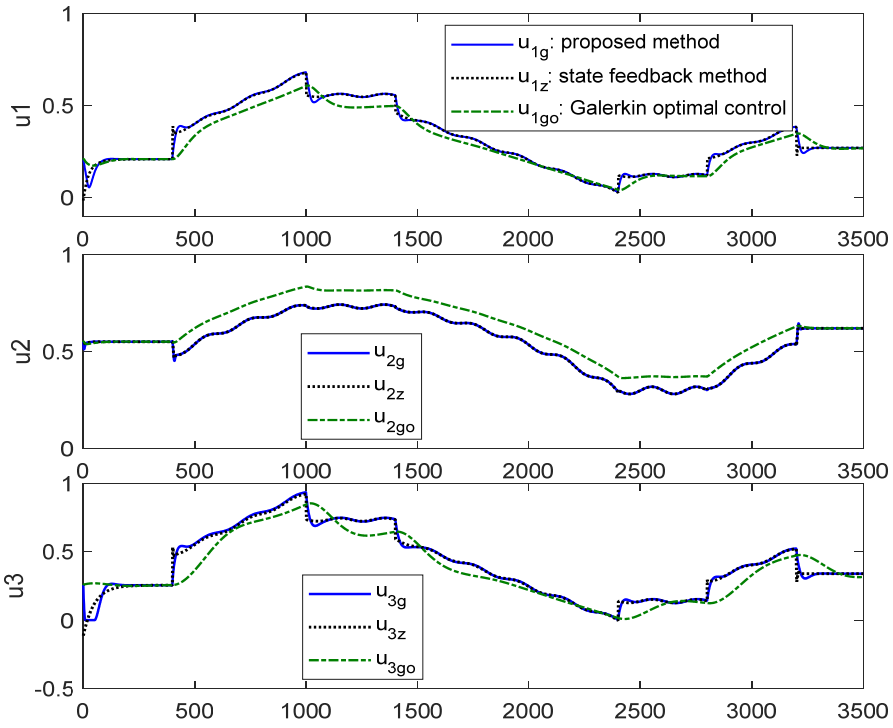

Figure 9. Control inputs in presence of lumped disturbances.

Figure 8 shows the output responses and Figure 9 gives the corresponding control inputs. Among them, y_{id}, $y_{ig}(u_{ig})$ and $y_{iz}(u_{iz})$ are setpoints, the outputs (inputs) produced by the proposed composite controller, and the outputs (inputs) produced by the comparative controller.

It can be noted from Figures 8 and 9 that the outputs of the two controllers can track the setpoints well with similar control inputs curves when the load changes over a wide range, indicating that the two control methods have similar disturbance rejection capability and can be adapted to large range load tracking scenarios. Moreover, for more clear comparisons, the following four-time frame are selected: (1) 1~100 s: the tracking process is of the set value under the initial deviation condition. (2) 390 s-480 s: the lumped disturbances occur and load starts to rise. (3) 990~1080 s: the lumped disturbances and the load begins to decline. (4) 3190~3280 s: the lumped disturbances disappear and the load begins to stabilize. The corresponding outputs and control inputs are illustrated in Figures 10–15.

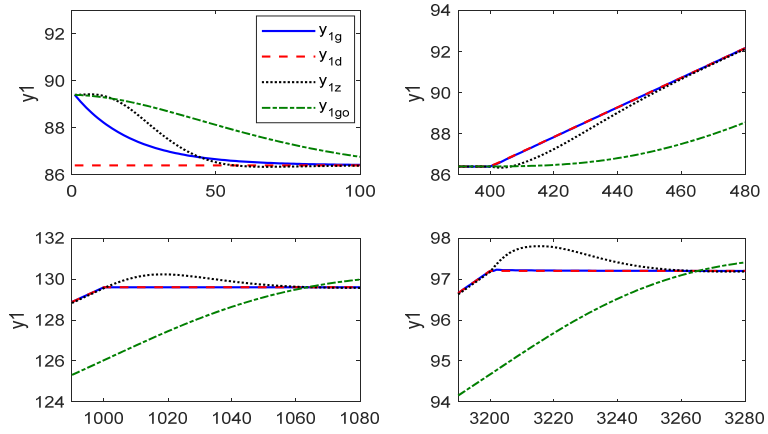

Figure 10. The comparison results of y_1 between the two controllers.

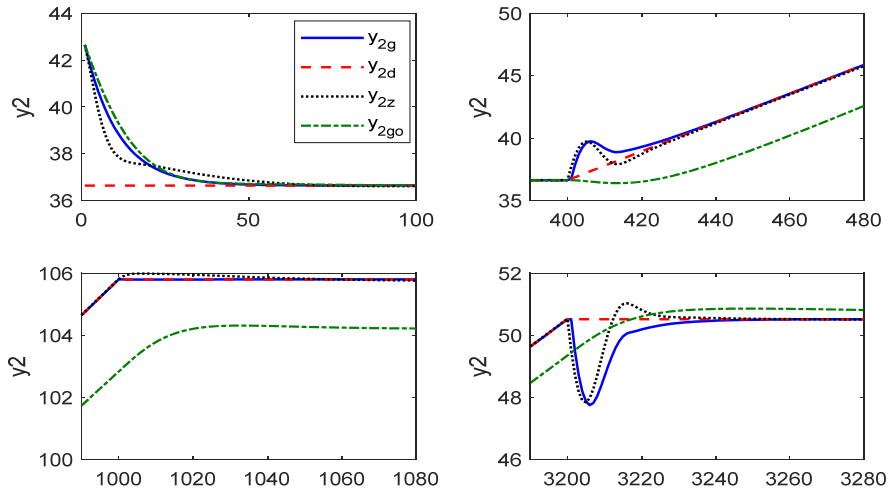

Figure 11. The comparison results of y_2 between the two controllers.

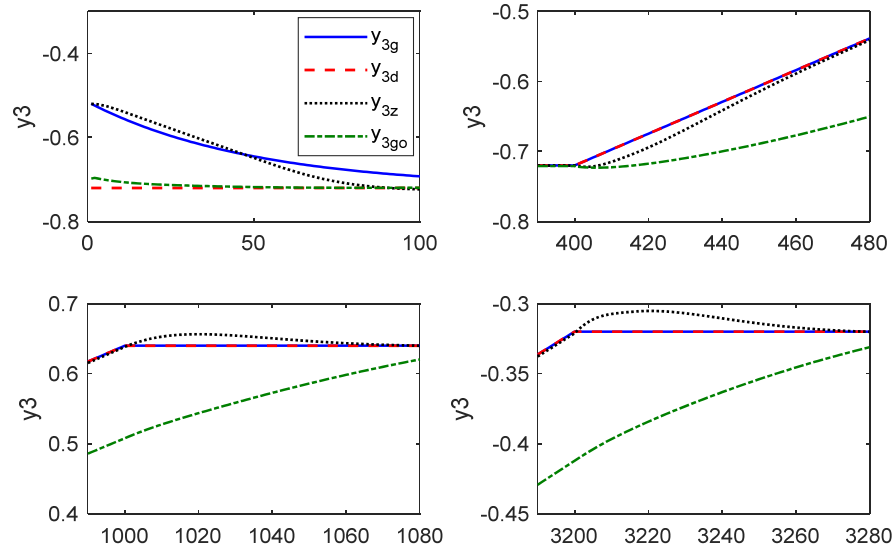

Figure 12. The comparison results of y_3 between the two controllers.

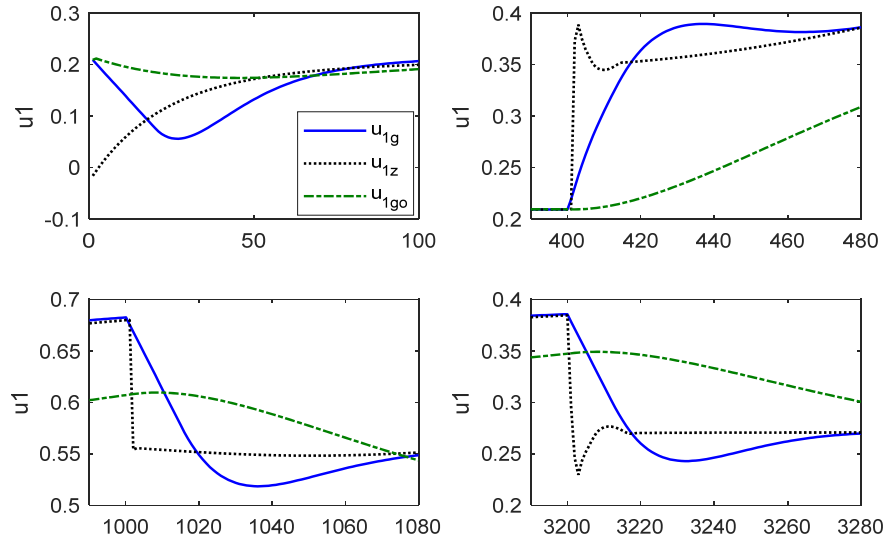

Figure 13. The comparison results of u_1 between the two controllers.

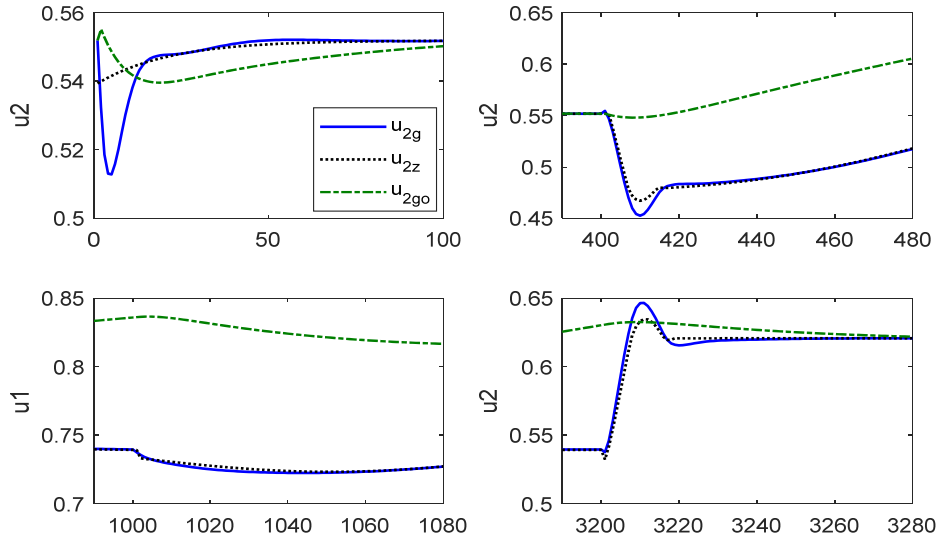

Figure 14. The comparison results of u_2 between the two controllers.

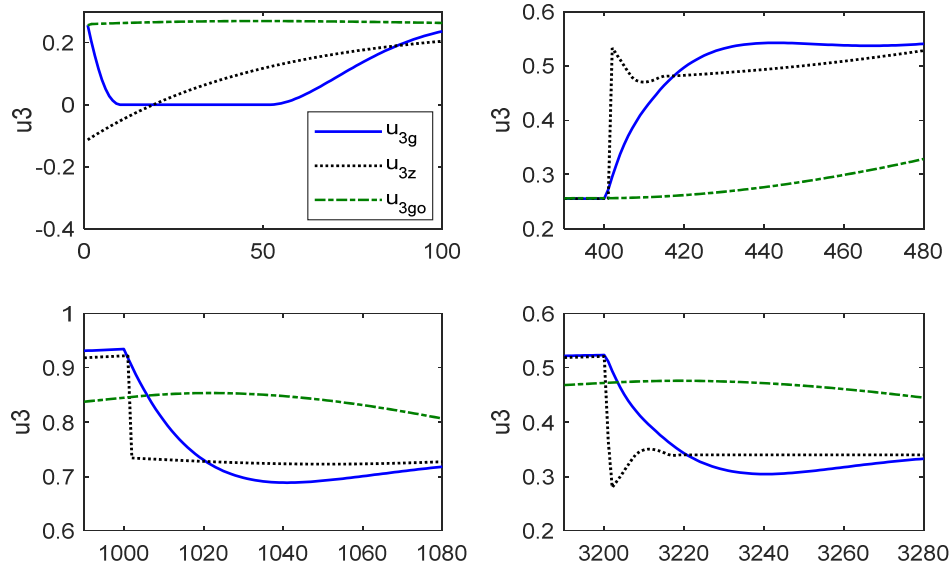

Figure 15. The comparison results of u_3 between the two controllers.

It can be concluded from Table 4 and Figures 10–15 that (i) the tracking rate of the comparative controller (y_{iz}) is faster than that of the proposed composite controller (y_{ig}), which means the rate of change of u_{iz} is higher than that of u_{ig}; (ii) When the deviation of initial condition setting is large, the initial stage of u_{3z} will be less than zero, which does not meet the constraint. However, the situation will not occur on the u_{3g} produced by the proposed composite controller due to the consideration of constraint during optimization; and (iii) the rate of change of the control input obtained by the comparative method is significantly higher than that of the proposed composite controller when the lumped disturbances occur, and the load starts to rise. This is due to the fact that the constraints of the input and output rates are taken into account in the controller design of the proposed control method while the constraints on control inputs are guaranteed by selecting reasonable state feedback controller's parameters of the comparative method. As a result, it is difficult to meet all constraints under the condition of severe disturbances of the comparative method. The IAE value of y_{3go} at all time frames are larger than the proposed method, because the disturbance rejection ability is weaker than the proposed one. Overall, the proposed method has a lower IAE index in each time frame compared with the other two methods.

Table 4. Quantitative integral absolute error (IAE) indexes of the simulation outputs.

($\mathbf{IAE}_{y_1}$,$\mathbf{IAE}_{y_2}$,$\mathbf{IAE}_{y_3}$)	**Time Frame (1)**	**Time Frame (2)**	**Time Frame (3)**	**Time Frame (4)**
Proposed method	(61.098, 63.04, 8.73)	(0.376, 26.6, 0.00105)	(0.0346,0.0472,0.000258)	(0.466, 29.64, 0.0027)
Galerkin control	(171.77, 72.39, 0.472)	(181.15, 219.023, 5.38)	(138.84, 165.61, 6.97)	(97.867, 39.399, 4.63)
State feedback control	(90.676, 60.343, 8.053)	(22.1, 25.217, 0.866)	(21.73, 6.45, 0.689)	(19.738, 25.095, 0.631)

According to the above comparison results, both controllers can fast-track the large-scale load. But the method proposed in [1] will result in control inputs that do not meet the constraints if the parameters are not selected properly or the disturbances are too severe. On the contrary, the presented receding Galerkin optimal controller with high-order sliding mode disturbance observer integrates the advantages of the high-order sliding mode disturbance observer and the receding Galerkin optimal control method, making it superior in constraint satisfaction, disturbance rejection, and large-scale load tracking.

5. Conclusions

In this paper, a receding Galerkin optimal controller with a high-order sliding mode disturbance observer is proposed to improve the control performance of a boiler-turbine unit. The presented controller can be directly designed based on the nonlinear mathematical unit model. More precisely, a high-order sliding mode disturbance observer is first employed to estimate the lumped disturbances and unmeasurable deviation states. Next, the estimate of the lumped disturbances is feedforward compensated in the receding optimization process. Then, based on the traditional Galerkin optimal control method, the idea of receding optimization is proposed to deal with lumped disturbances, variable constraints, and large-scale load tracking at the same time. Simulation results have shown that the proposed controller can regulate the boiler-turbine unit to track large-scale load set-points and meet the variable constraints in the presence of various types of unknown disturbances.

6. Annexe

All the necessary variables of controlled boiler–turbine unit by proposed method are listed in Table 5 for the easy of query.

Table 5. Variable of Controlled Boiler–Turbine Unit.

Variable	a_1~a_3	b_1~b_3	c_1~c_4	α_{cs}
Name	identified parameter	identified parameter	identified parameter	coefficient
	x_1	x_2	x_3	y_1
	drum pressure	electrical output	fluid density in the drum	drum steam pressure
	y_2	y_3	u_1	u_2
	electrical output	drum water level	valve positions for fuel	valve positions for steam
	u_3	q_e	$\overline{d}_i(t),\ i = 1,2,3$	$x_{1d} \sim x_{3d}$
	valve positions for feedwater flow	evaporation rate of steam	unknown disturbances	setpoint signal for state
	$u_{1d} \sim u_{3d}$	y_{3d}	$w(t)$	$d_1(t) \sim d_3(t)$
	setpoint signal for input	setpoint signal for output	disturbance term	lumped disturbance
	$v_1 \sim v_3$	$z_1 \sim z_3$	$\xi_0^i \sim \xi_L^i$	J_{BT}
	virtual control law	states/outputs error	HOSMO estimate	cost function
	$L_N(\tau)$	z^{N_j}	u^{N_j}	
	Nth order Legendre polynomial	state variables at the LGL nodes	control variables at the LGL nodes	

Author Contributions: Conceptualization, Z.-G.S. and G.Z.; methodology, Z.-G.S.; software, G.Z.; validation, G.Z. and Y.H.; formal analysis, Y.S.; investigation, G.Z.; resources, Z.-G.S. and G.Z.; data curation, Y.H.; writing—original draft preparation, G.Z.; writing—review and editing, Y.S.; visualization, G.Z. and Y.S.; supervision, Z.-G.S.; project administration, Z.-G.S.; funding acquisition, Z.-G.S. All authors have read and agreed to the published version of the manuscript.

Funding: This research was funded by the National Natural Science Foundation of China, grant number 52076037.

Institutional Review Board Statement: Not applicable.

Informed Consent Statement: Not applicable.

Data Availability Statement: The data that support the findings of this study are available on request from the corresponding author, upon reasonable request.

Conflicts of Interest: The authors declare no conflict of interest.

References

1. Su, Z.G.; Zhao, G.; Yang, J.; Li, Y.G. Rejection of Nonlinear Boiler-Turbine Unit Using High-Order Sliding Mode Observer. *IEEE Trans. Syst. Man Cybern. -Syst.* **2018**, *50*, 5432–5443. [CrossRef]
2. Xu, Z.Y.; Qu, H.N.; Shao, W.H.; Xu, W.S. Virtual power plant based pricing control for wind/thermal cooperated generation in China. *IEEE Trans. Syst. Man Cybern. -Syst.* **2016**, *46*, 706–712. [CrossRef]
3. Zhang, S.; Taft, C.W.; Bentsman, J.; Hussey, A.; Petrus, B. Simultaneous gains tuning in boiler/turbine PID-based controller clusters using iterative feedback tuning methodology. *ISA Trans.* **2012**, *51*, 609–621. [CrossRef]
4. Yang, S.; Qian, C.; Du, H. A genuine nonlinear approach for controller design of a boiler–turbine system. *ISA Trans.* **2012**, *51*, 446–453. [CrossRef]
5. Fang, F.; Wei, L. Backstepping-based nonlinear adaptive control for coal-fired utility boiler–turbine units. *Appl. Energy* **2011**, *88*, 814–824. [CrossRef]
6. Chen, P.C.; Shamma, J.S. Gain-scheduled ℓ1-optimal control for boiler-turbine dynamics with actuator saturation. *J. Process Control.* **2004**, *14*, 263–277. [CrossRef]
7. Ghabraei, S.; Moradi, H.; Vossoughi, G. Multivariable robust adaptive sliding mode control of an industrial boiler–turbine in the presence of modeling imprecisions and external disturbances: A comparison with type-I servo controller. *ISA Trans.* **2015**, *58*, 398–408. [CrossRef]
8. Sariyildiz, E.; Oboe, R.; Ohnishi, K. Disturbance observer-based robust control and its applications: 35th anniversary overview. *IEEE Trans. Ind. Electron.* **2020**, *67*, 2042–2053. [CrossRef]
9. Morales, J.Y.R.; Mendoza, J.A.B.; Torres, G.O.; Vázquez, F.D.J.S.; Rojas, A.C.; Vidal, A.F.P. Fault-Tolerant Control implemented to Hammerstein–Wiener model: Application to Bio-ethanol dehydration. *Fuel* **2022**, *308*, 121836. [CrossRef]
10. Ortiz Torres, G.; Rumbo Morales, J.Y.; Ramos Martinez, M.; Valdez-Martínez, J.S.; Calixto-Rodriguez, M.; Sarmiento-Bustos, E.; Torres Cantero, C.A.; Buenabad-Arias, H.M. Active Fault-Tolerant Control Applied to a Pressure Swing Adsorption Process for the Production of Bio-Hydrogen. *Mathematics* **2023**, *11*, 1129. [CrossRef]
11. Morales, J.Y.R.; López, G.L.; Martínez, V.M.A.; Vázquez, F.D.J.S.; Mendoza, J.A.B.; García, M.M. Parametric study and control of a pressure swing adsorption process to separate the water-ethanol mixture under disturbances. *Sep. Purif. Technol.* **2020**, *236*, 116214. [CrossRef]
12. Chen, P.C. Multi-objective control of nonlinear boiler-turbine dynamics with actuator magnitude and rate constraints. *ISA Trans.* **2013**, *52*, 115–128. [CrossRef]
13. Li, Y.; Shen, J.; Lee, K.Y.; Liu, X. Offset-free fuzzy model predictive control of a boiler–turbine system based on genetic algorithm. *Simul. Model. Pract. Theory* **2012**, *26*, 77–95. [CrossRef]
14. Kong, X.; Liu, X.; Lee, K.Y. Nonlinear multivariable hierarchical model predictive control for boiler-turbine system. *Energy* **2015**, *93*, 309–322. [CrossRef]
15. Ławryńczuk, M. Nonlinear predictive control of a boiler-turbine unit: A state-space approach with successive on-line model linearisation and quadratic optimisation. *ISA Trans.* **2017**, *67*, 476–495. [CrossRef]
16. Wu, X.; Shen, J.; Li, Y.; Lee, K.Y. Data-driven modeling and predictive control for boiler–turbine unit using fuzzy clustering and subspace methods. *ISA Trans.* **2014**, *53*, 699–708. [CrossRef]
17. Liu, X.; Kong, X. Nonlinear fuzzy model predictive iterative learning control for drum-type boiler–turbine system. *J. Process Control* **2013**, *23*, 1023–1040. [CrossRef]
18. Yang, S.; Qian, C. Real-time optimal control of a boiler-turbine system using pseudospectral methods. In Proceedings of the 19th Annual Joint ISA POWID/EPRI Controls and Instrumentation Conference and 52nd ISA POWID Symposium, Rosemont, IL, USA, 12–14 May 2009; Volume 477, pp. 166–177.
19. Elnagar, G.; Kazemi, M.A.; Razzaghi, M. The pseudospectral Legendre method for discretizing optimal control problems. *IEEE Trans. Autom. Control* **1995**, *40*, 1793–1796. [CrossRef]

20. Biegler, L.T. Nonlinear programming: Concepts, algorithms, and applications to chemical processes. In *Society for Industrial and Applied Mathematics*; SIAM: Philadelphia, PA, USA, 2010. [CrossRef]
21. Boucher, R.; Kang, W.; Gong, Q. Galerkin optimal control for constrained nonlinear problems. In Proceedings of the 2014 American Control Conference, Portland, OR, USA, 4–6 June 2014; pp. 2432–2437.
22. Boucher, R.; Kang, W.; Gong, Q. Galerkin optimal control. *J. Optim. Theory Appl.* **2016**, *169*, 825–847. [CrossRef]
23. Zhao, G.; Su, Z.G.; Zhan, J.; Zhu, H.; Zhao, M. Adaptively receding Galerkin optimal control for a nonlinear boiler-turbine unit. *Complexity* **2018**, *2018*, 8643623. [CrossRef]
24. Xu, B. Disturbance observer-based dynamic surface control of transport aircraft with continuous heavy cargo airdrop. *IEEE Trans. Syst. Man Cybern. Syst.* **2016**, *47*, 161–170. [CrossRef]
25. Yang, J.; Liu, X.; Sun, J.; Li, S. Sampled-data robust visual servoing control for moving target tracking of an inertially stabilized platform with a measurement delay. *Automatica* **2022**, *137*, 110105. [CrossRef]
26. Li, S.; Yang, J.; Chen, W.H.; Chen, X. *Disturbance Observer-Based Control: Methods and Applications*; CRC Press: Boca Raton, FL, USA, 2014.
27. Han, J. From PID to active disturbance rejection control. *IEEE Trans. Ind. Electron.* **2009**, *56*, 900–906. [CrossRef]
28. Madonski, R.; Łakomy, K.; Stankovic, M.; Shao, S.; Yang, J.; Li, S. Robust converter-fed motor control based on active rejection of multiple disturbances. *Control Eng. Pract.* **2021**, *107*, 104696. [CrossRef]
29. Gao, Z. Scaling and bandwidth-parameterization based controller tuning. *ACC* **2003**, 4989–4996.
30. Gao, X.H.; Wei, S.; Wang, M.; Su, Z.G. Optimal disturbance predictive and rejection control of a parabolic trough solar field. *Int. J. Robust Nonlinear Control*, 2023; *in press*. [CrossRef]
31. Zhang, F.; Wu, X.; Shen, J. Extended state observer based fuzzy model predictive control for ultra-supercritical boiler-turbine unit. *Appl. Therm. Eng.* **2017**, *118*, 90–100. [CrossRef]
32. Zeng, L.; Li, Y.; Liao, P.; Wei, S. Adaptive disturbance rejection model predictive control and its application in a selective catalytic reduction denitrification system. *Comput. Chem. Eng.* **2020**, *140*, 106963. [CrossRef]
33. Bell, R.D.; Åström, K.J. *Dynamic models for Boiler-Turbine-Alternator Units: Data Logs and Parameter Estimation for a 160 MW Unit*; Research Reports TFRT-3192; Department of Automatic Control, Lund Institute of Technology (LTH): Lund, Sweden, 1987.
34. Levant, A. Higher-order sliding modes, differentiation and output-feedback control. *Int. J. Control* **2003**, *76*, 924–941. [CrossRef]
35. Shtessel, Y.B.; Shkolnikov, I.A.; Levant, A. Smooth second-order sliding modes: Missile guidance application. *Automatica* **2007**, *43*, 1470–1476. [CrossRef]
36. Li, S.; Sun, H.; Yang, J.; Yu, X. Continuous finite-time output regulation for disturbed systems under mismatching condition. *IEEE Trans. Autom. Control* **2014**, *60*, 277–282. [CrossRef]
37. Gill, P.E.; Murray, W.; Saunders, M.A. SNOPT: An SQP algorithm for large-scale constrained optimization. *SIAM Rev.* **2005**, *47*, 99–131. [CrossRef]
38. Zhan, J.; Su, Z.; Hao, Y. Optimal control for a boiler-turbine system via Galerkin method. In Proceedings of the 2017 2nd International Conference on Power and Renewable Energy (ICPRE), Chengdu, China, 20–23 September 2017; pp. 776–780.
39. Gong, Q.; Kang, W.; Ross, I.M. A pseudospectral method for the optimal control of constrained feedback linearizable systems. *IEEE Trans. Autom. Control* **2006**, *51*, 1115–1129. [CrossRef]